Electronic Supporting Information for:

Preparation of Highly Dispersed γ-Fe_2O_3 and $GdPO_4$ Co-Functionalized Mesoporous Carbon Spheres for Dual-mode MR Imaging and Anti-cancer Drug Carrying

Qianqian Zhang, Peiyuan Wang, Xiaomin Li, Yongtai Yang, Xiaofeng Liu, Fan Zhang, Yun Ling* and Yaming Zhou*

Shanghai Key Laboratory of Molecular Catalysis and Innovative Materials, Department of Chemistry, Fudan University, Shanghai, 200433, China.

*E-mail: yunling@fudan.edu.cn and ymzhou@fudan.edu.cn

Experimental Section

Materials: Poly (ethylene oxide)-block-poly (propylene oxide) block-poly-(ethylene oxide) triblock copolymer Pluronic F127 (Mw = 12600, $PEO_{106}PPO_{70}PEO_{106}$) was purchased from Acros Corp. $Fe(NO_3)_3 \cdot 9H_2O$, $Gd(NO_3)_3 \cdot 6H_2O$, Gd_2O_3, pivalic acid, phenylphosphonic acid, MeCN (acetonitrile), trimethylamine, phenol, formalin solution (37 wt%), sodium hydroxide, tetrahydrofuran (THF), ethanol (EtOH), aether (Et_2O), toluene ($PhCH_3$), $CHCl_3$, N, N-dimethylformamide (DMF) and doxorubicin hydrochloride (DOX) were purchased from Aladdin. Fluorescein isothiocyanate (FITC) was purchased from Macklin. DMEM (dulbecco minimum essential medium) solution, DAPI (4',6-diamidino-2-phenylindole). All chemicals were used as received without any further purification.

Characterization: Thermal stability studies were carried out on a Mettler Tolepo TGA/SDTA 851 thermoanalyzer under N_2 flow from 30 to 650 °C at a heating rate of 10 $^oC\ min^{-1}$. Powder X-ray diffraction (PXRD) data were recorded on a Bruker D8 Advance diffractometer at 40 kV, 40 mA with Cu−Kα radiation (λ = 1.5406 Å). Small angle X-ray scattering (SAXS) measurements were taken on a Nanostar U SAXS system (Bruker, Germany) using Cu Kα radiation (40 kV, 35 mA). The *d*-spacing values were calculated using the formula $d = 2\pi/q$, and the unit cell parameters were calculated with the formula $a = (\sqrt{2})d_{110}$. The pore wall thicknesses were calculated from the formula $h = (\sqrt{3})a/2\text{-}D$.[1] Transmission electron microscopy (TEM) measurements were conducted on a JEM-2100 microscope (JEOL, Japan) operated at 200 kV. N_2 sorption at –196 °C was measured on an ASAP 2020 gas adsorption apparatus (Micromeritics). Before gas absorption, the samples were degassed in a vacuum at 300 °C for 10 h. The UV–vis absorbance spectra were collected by a Perkin Elmer UV Spectrometer Lambda 750S. Confocal images of the cells were

performed with an Olympus FV1000 laser scanning confocal microscope and a 60 × oil-immersion objective lens.

Preparation of {$Fe_6Gd_6P_6$} Cluster: $[Fe_6Gd_6(\mu_3\text{-}O)_2(CO_3)(O_3PPh)_6(O_2C^tBu)_{18}]$ ({$Fe_6Gd_6P_6$} for short) was prepared as described previously.[2] A mixture of $[Fe^{III}_3(\mu_3\text{-}O)(O_2C^tBu)_6(HO_2C^tBu)_3](O_2C^tBu)$[3,4] (0.09 g, 0.075 mmol), $[Gd^{III}_2(O_2C^tBu)_6(HO_2C^tBu)_6]$[5] (0.15 g, 0.1 mmol), $C_6H_5PO_3H_2$ (0.016 g, 0.1 mmol), triethylamine (0.14 mL, 1 mmol) and acetonitrile (8 mL) was placed in a 10 mL Teflon-lined autoclave and was stirred at room temperature for 5 min. The mixture was then heated at 150 °C for 12 h, followed by cooling down to the room temperature. Reddish-brown crystals were collected by filtration. Yield: 40 % (based on $C_6H_5PO_3H_2$).

Synthesis of spherical F127/resol composites with ordered cubic mesostructured: The mesoporous polymers were prepared according to the literature method.[6] In a typical synthesis, 0.6 g of phenol, 2.1 ml of formalin aqueous solution (37 wt %) and 15 ml of (0.1 M) NaOH aqueous solution were mixed and stirred at 70 °C for 0.5 h to obtain low-molecular-weight phenolic resols. After that, 0.96 g of triblock copolymer Pluronic F127 dissolved in 15 ml of H_2O was added. Then the mixture was stirred at 66 °C with a stirring speed of 340 ± 40 rpm for 2 h. After that, 50 ml water was added to dilute the solution. During this reaction, the color of the aqueous solution was turned from colorless transparent to pink and finally turned to crimson. After 16–18 h, the reaction was stopped when the deposit was observed. After quiescence until the deposit was dissolved, 17.7 ml of the obtained solution was transferred into an autoclave and diluted with 56 ml of H_2O and heated at 130 °C for 24 h. The products were collected by centrifugation and washed with distilled water for several times and dried at room temperature.

Synthesis of ordered-mesoporous carbon spheres (OMCS) functionalized by *γ*-Fe_2O_3 and $GdPO_4$ nanoparticles (Fe–Gd/OMCSs): Typically, 9 mg of $\{Fe_6Gd_6P_6\}$ clusters were dissolved in the 2 ml of ethanol. Then 20 mg of the spherical F127/resol composites obtained above were added with stirring at room temperature until ethanol was full evaporated. The as-made $\{Fe_6Gd_6P_6\}$–F127/resol samples were calcined under N_2 atmosphere at 600 ^oC for 3 h with a temperature ramp of 1 ^oC min^{-1}, denoted as Fe–Gd/OMCS-45 (Fe–Gd/OMCS-*n*, $n = (W_{cluster} / W_{F127/resol}) \times 100$). The same procedures were carried out for the preparation of composites Fe–Gd/OMCS-15, Fe–Gd/OMCS-30, Fe–Gd/OMCS-60 and Fe–Gd/OMCS-75 except that the amounts of $\{Fe_6Gd_6P_6\}$ clusters were 3, 6, 12 and 15 mg, respectively.

For comparison, $Fe(NO_3)_3 \cdot 9H_2O$, $Gd(NO_3)_3 \cdot 6H_2O$ and phenylphosphonic acid were directly used as metal precursors for preparing functionalized ordered mesoporous carbon spheres under the same conditions as the Fe–Gd/OMCS-45 composite. It was designated as Fe–Gd/OMCS-45-i.

Post-synthetic method for functionalization of OMCSs by $\{Fe_6Gd_6P_6\}$ was carried out. Typically, 20 mg of the spherical F127/resol composites obtained above were carbonized at 600 ^oC for 3 h under N_2 atmosphere to form OMCSs. Then they were uniformly dispersed in the ethanol solution containing 9 mg of $\{Fe_6Gd_6P_6\}$. The mixed solution was stirred at room temperature until ethanol was full evaporated. The as-loaded $\{Fe_6Gd_6P_6\}$/OMCSs were further calcined under N_2 atmosphere at 600 ^oC for 3 h with a temperature ramp of 1 °C min^{-1}, named as Fe–Gd/OMCS-45-ii.

T_1 and T_2 relaxivity measurement of Fe–Gd/OMCS-45-air *in vitro*: T_1- and T_2-weighted MR imaging experiment *in vitro* was performed on a 0.5 T clinical MR imaging instrument (MesoMR23-060H-I). For *in vitro* MR images and both T_1 and T_2 measurements, Fe–Gd/OMCS-

45-air was dispersed in the deionized water at various gadolinium (iron) concentrations (0.02511, 0.05023, 0.1004, 0.2009, 0.4018 and 0.8035 mmol L^{-1}). T_1-weighted MR images were acquired using a conventional spin-echo sequence under the following parameters: TR/TE = 180/15 ms, 256 × 192 matrices, 100 × 100 mm^2 field of view, Sweep Width (SW) = 20 KHz , a slice thickness of 5 mm. T_2-weighted MR images using a fast spin-echo sequence was used to reduce acquisition time under the following parameters: TR/TE = 3000/110 ms, 256 × 192 matrices, 100 × 100 mm^2 field of view, Sweep Width (SW) = 20 KHz, a slice thickness of 5 mm. The specific relaxivity values of r_1 and r_2 were calculated through the curve fitting of $1/T_1$ and $1/T_2$ (s^{-1}) vs the composites concentration (mM).

Drug loading: 10 mg Fe–Gd/OMCS-45-air materials dispersed in 2 mL phosphate buffered saline (PBS) solution with fixed concentration of DOX (1 mg ml^{-1}). Then the mixture was stirred for about 12 h at room temperature under dark conditions. The DOX-loaded sample was collected by centrifugation and washed by PBS solution. The supernatant and washed solutions were collected. The residual concentration of DOX was determined by UV/VIS spectrophotometer at the maximum absorbance of 481 nm. Repeat these steps for the DOX-loaded Fe–Gd/OMCS-45-air until the DOX concentration of the solution was steady.

Cellular uptake evaluation: 10 mg of Fe–Gd/OMCS-45-air and 0.1 mg of fluorescein isothiocyanate (FITC) were dispersed in tetrahydrofuran (THF, 5 mL) by ultrasonication, and the mixture solution was stirred at 30 °C for 6 h. Then the sample FITC labeled Fe–Gd/OMCS-45-air was washed with PBS solution for several times until the eluate could not inspect any fluorescein. HeLa cells (5×10^4) well seeded on a culture dish for 24 h. Then cell culture medium was changed to fresh DMEM (dulbecco minimum essential medium) solution with FITC labeled Fe–Gd/OMCS-45-air (100 μg mL^{-1}). After incubating for 1 h at 37 °C, the cells were rinsed three times with PBS,

followed by fixing with Paraformaldehyde solution for 15 min at 4 ^{o}C. Finally, the nuclei were stained by DAPI (4',6-diamidino-2-phenylindole) (1 μg ml^{-1}). Then the cells were washed using PBS solution twice. The fluorescence behavior was measured under 488 nm, 405 nm laser for FITC and DAPI, respectively. Emission for FITC and DAPI was collected from 425–525 nm and 550–650 nm.

Following the same procedure, the Hela cells were treated with the DOX@Fe–Gd/OMCS-45-air for different time periods (1, 2 and 4 h). The cells with DOX@ Fe–Gd/OMCS-45-air incubation were excited at 488 nm and emission was collected from 580 to 680 nm.

Cell Cytotoxicity: Cell Counting Kit-8 (CCK-8) assay was used to evaluate the cytotoxicity of the Fe–Gd/OMCS-45-air and DOX@Fe–Gd/OMCS-45-air materials on HeLa cells. HeLa cells were harvested by trypsinization and seeded into 96-well cell-culture plate at 1 × 10^{4}/well and incubated for 24 h at 37 °C under 5 % CO_2. Then HeLa cells were co-cultured with 1–300 μg ml^{-1} of the Fe–Gd/OMCS-45-air and DOX@Fe–Gd/OMCS-45-air materials for 4 h, respectively. The kit of CCK-8 was then (10 μL/well) added to each well and incubated at 37 °C for 2 h. Enzyme dehydrogenase in living cells was oxidized by this kit to orange carapace. The quality was assessed calorimetrically by using a multi-reader (TECAN, Infinite M200, Germany). The measurements were based on the absorbance values at 450 nm. Following formula was used to calculate the viability of cell growth:

Viability (%) = (mean absorbance value of treatment group/mean absorbance value of control group) × 100.

Following the same procedure, HeLa cells were co-cultured with 1–300 μg ml^{-1} of the Fe–Gd/OMCS-45-air and DOX@Fe–Gd/OMCS-45-air materials for 24 h, respectively. Then the cell livability was calculated.

In vitro **MR images of cells:** Hela cells were incubated with DOX@Fe–Gd/OMCS-45-air materials with different concentrations for 4 h in 37 ^{o}C. After incubation, the cells were washed with PBS buffer three times and resuspended in PBS buffer before MR imaging. All MR imaging measurements were performed with a 0.5 T systems (MesoMR23-060H-I).

Figure S1. (a) Crystal structure of $\{Fe_6Gd_6P_6\}$ cluster. (b) Polyhedral representation of $\{Fe_6Gd_6P_6\}$ core.

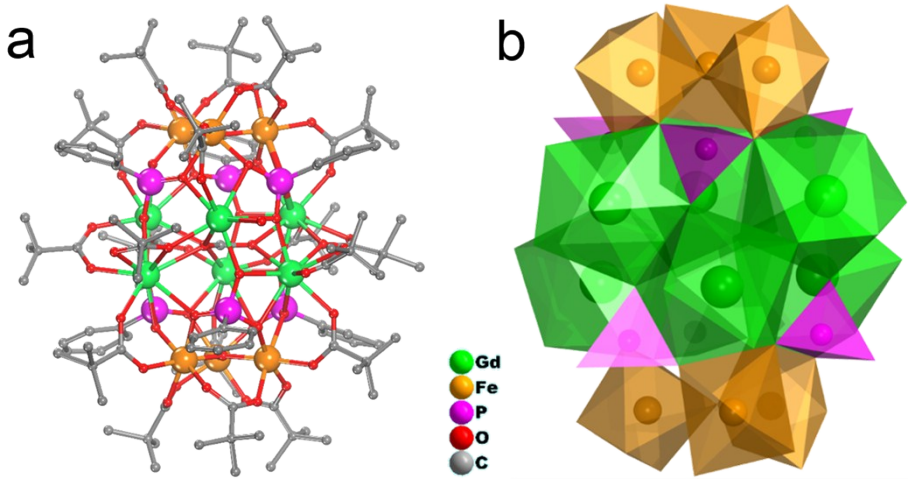

Figure S2. The solubility of $\{Fe_6Gd_6P_6\}$ in the following solvents: H_2O, EtOH, THF, Et_2O, $PhCH_3$, $CHCl_3$, DMF.

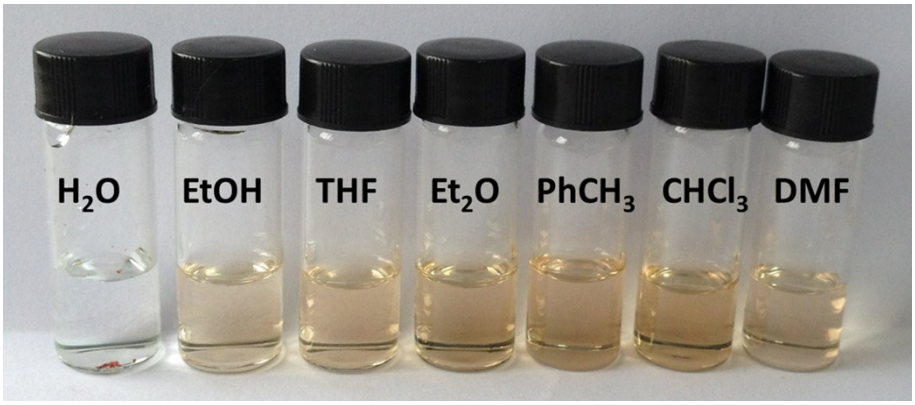

Figure S3. (a) The TGA data of $\{Fe_6Gd_6P_6\}$ clusters under N_2 and air flow from 35 °C to 650 °C. (b) Temperature-dependent PXRD patterns of $\{Fe_6Gd_6P_6\}$ clusters.

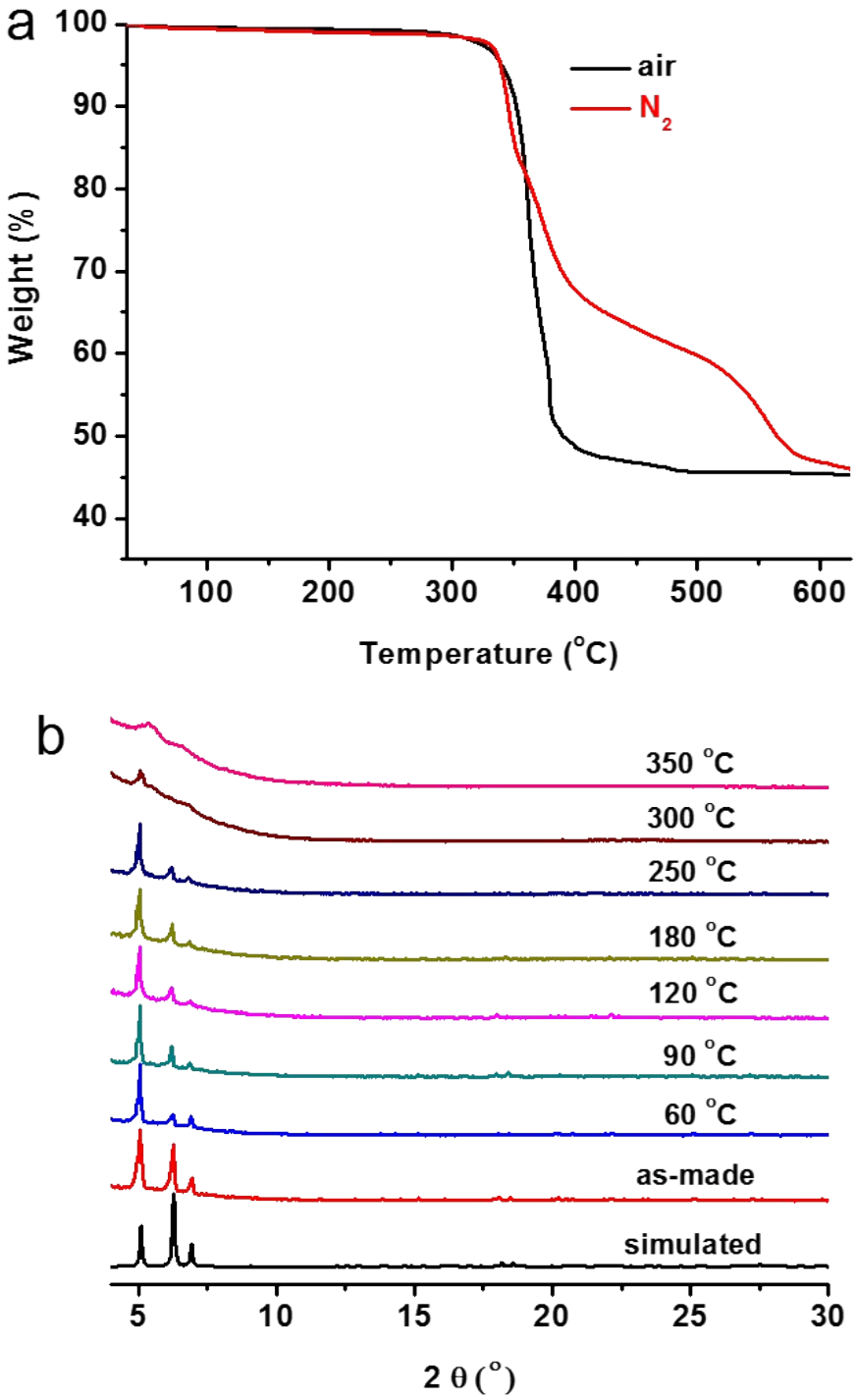

Figure S4. PXRD pattern of residue compounds of $\{Fe_6Gd_6P_6\}$ clusters calcinated at 600 °C under nitrogen atmosphere.

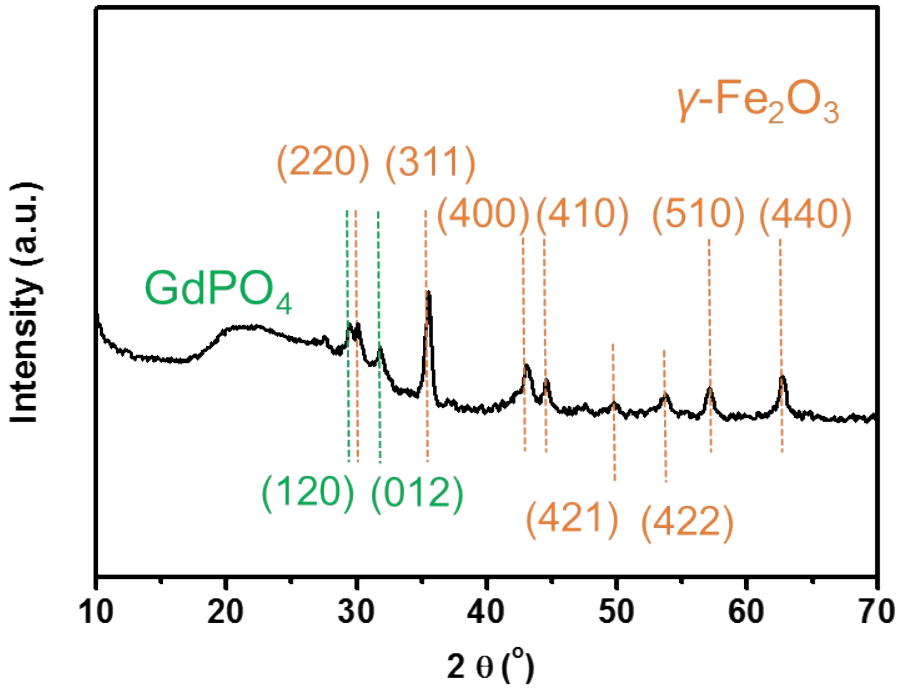

Figure S5. (a) N_2 adsorption−desorption isotherm and the corresponding pore size distribution of as-made spherical F127/resol composites, (b) FT-IR absorption spectra of F127/resol, $\{Fe_6Gd_6P_6\}$ and $\{Fe_6Gd_6P_6\}$–F127/resol.

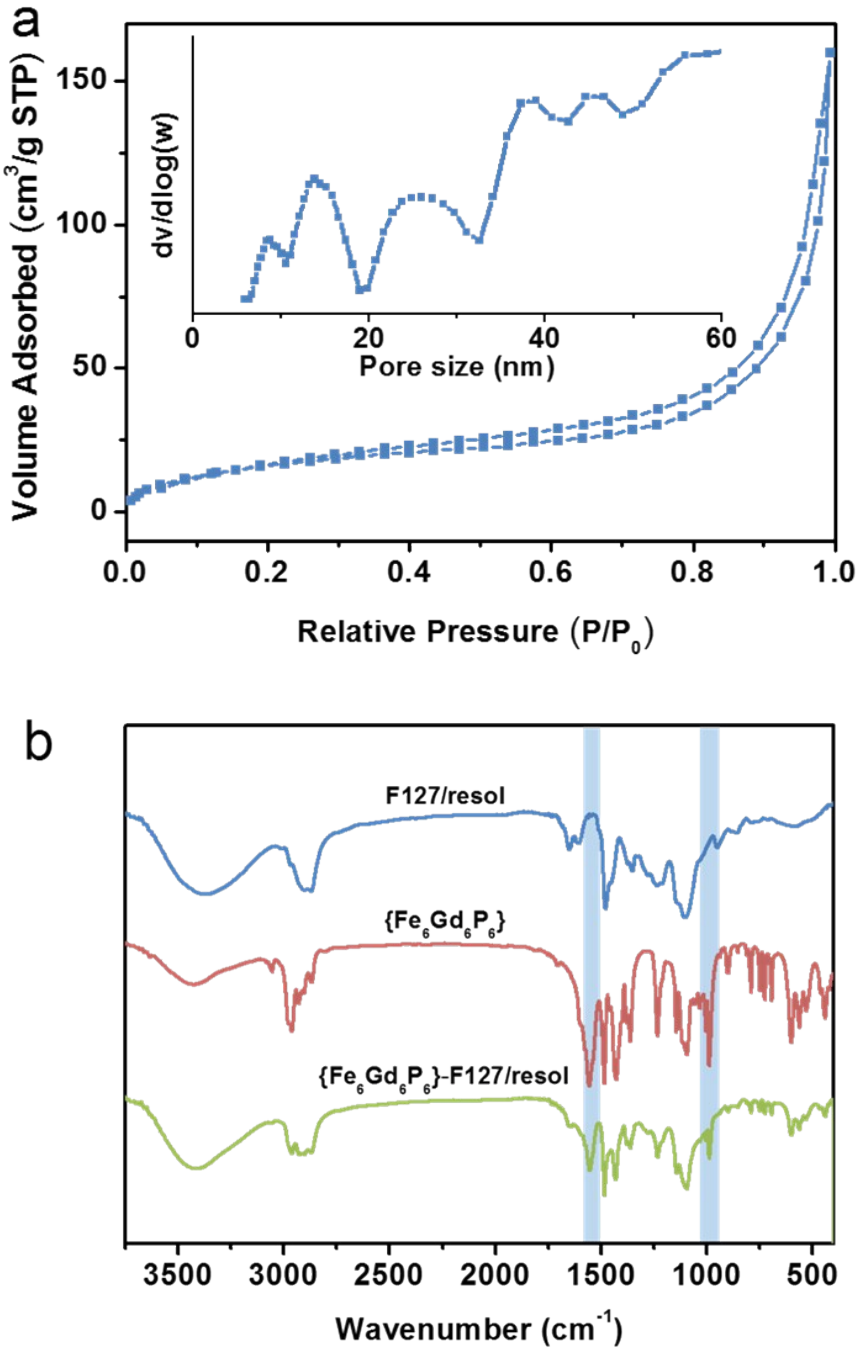

Figure S6. SAXS patterns of as-made functionalized F127/resol composites: (I) OMCS-as-made, (II) Fe–Gd/OMCS-15-as-made, (III) Fe–Gd/OMCS-30-as-made, (IV) Fe–Gd/OMCS-45-as-made, (V) Fe–Gd/OMCS-60-as-made and (VI) Fe–Gd/OMCS-75-as-made.

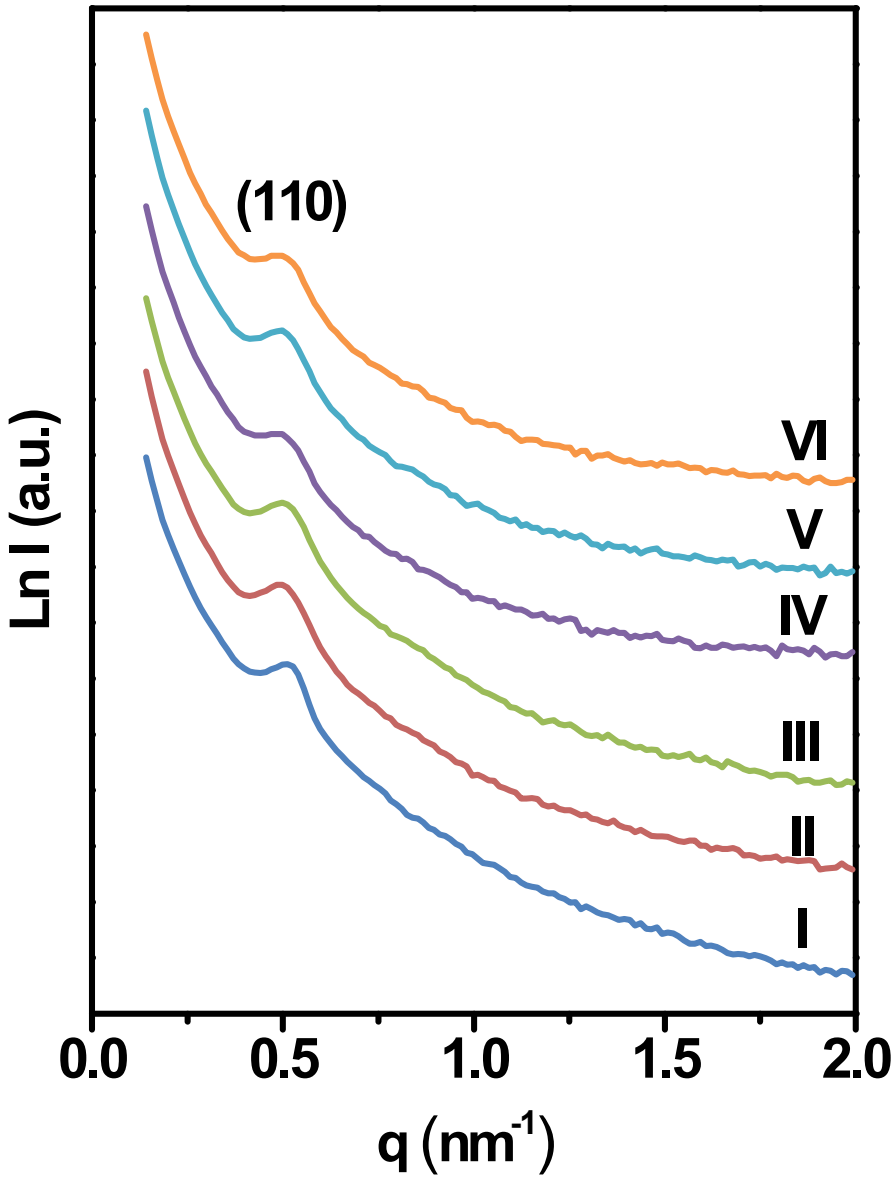

Figure S7. (a) SAXS patterns and (b) N_2 adsorption−desorption isotherms and the corresponding pore size distributions of Fe–Gd/OMCS-*n*: (I) OMCSs, (II) Fe–Gd/OMCS-15, (III) Fe–Gd/OMCS-30, (IV) Fe–Gd/OMCS-45, (V) Fe–Gd/OMCS-60 and (VI) Fe–Gd/OMCS-75.

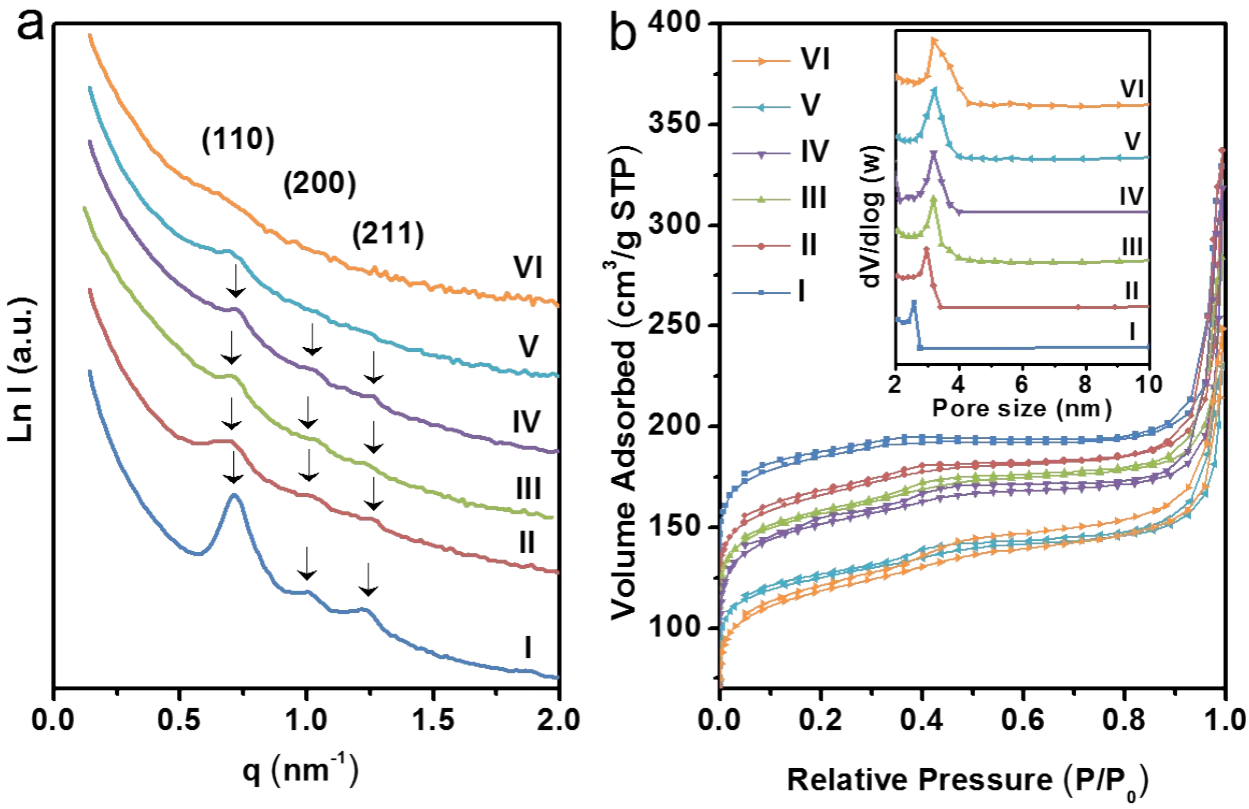

Figure S8. PXRD patterns of Fe–Gd/OMCS-*n*: (I) Fe–Gd/OMCS-15, (II) Fe–Gd/OMCS-30, (III) Fe–Gd/OMCS-45, (IV) Fe–Gd/OMCS-45-air, (V) Fe–Gd/OMCS-60 and (VI) Fe–Gd/OMCS-75.

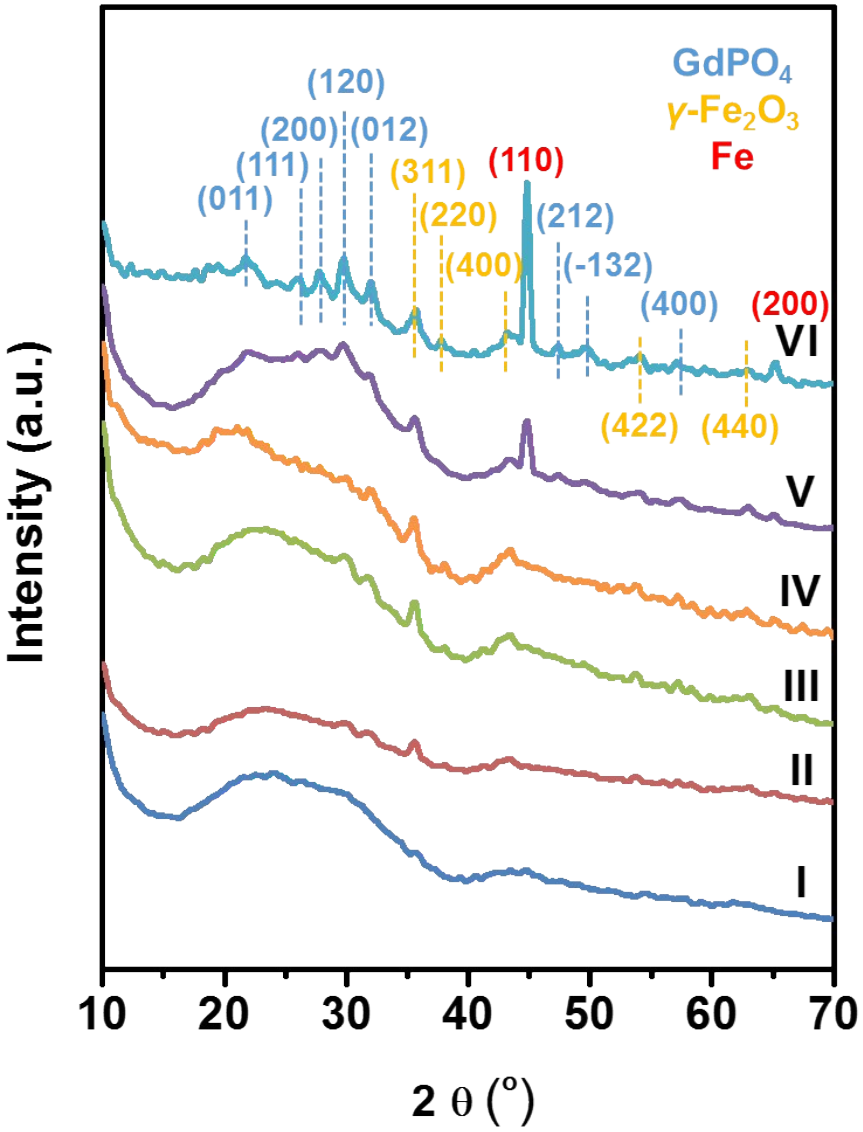

Figure S9. Fe–Gd/OMCS-15 composites: (a) HAADF-STEM image, (b) overlay maps of C, O, Gd, P and Fe elements, the corresponding EDS maps of (c) C, (d) O, (e) Gd, (f) P, (g) Fe and (h) the corresponding element analysis result.

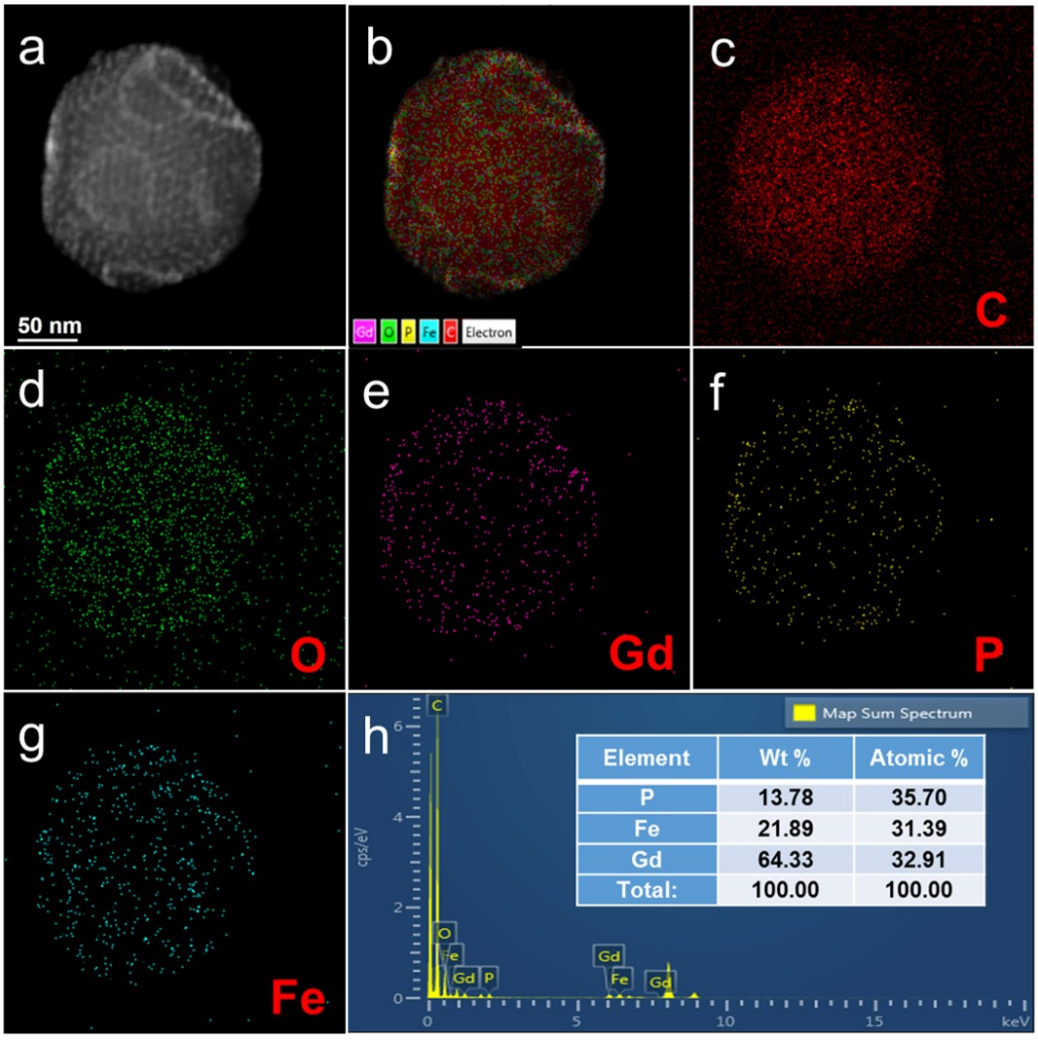

Figure S10. Fe–Gd/OMCS-30 composites: (a) HAADF-STEM image, (b) overlay maps of C, O, Gd, P and Fe elements, the corresponding EDS maps of (c) C, (d) O, (e) Gd, (f) P, (g) Fe and (h) the corresponding element analysis result.

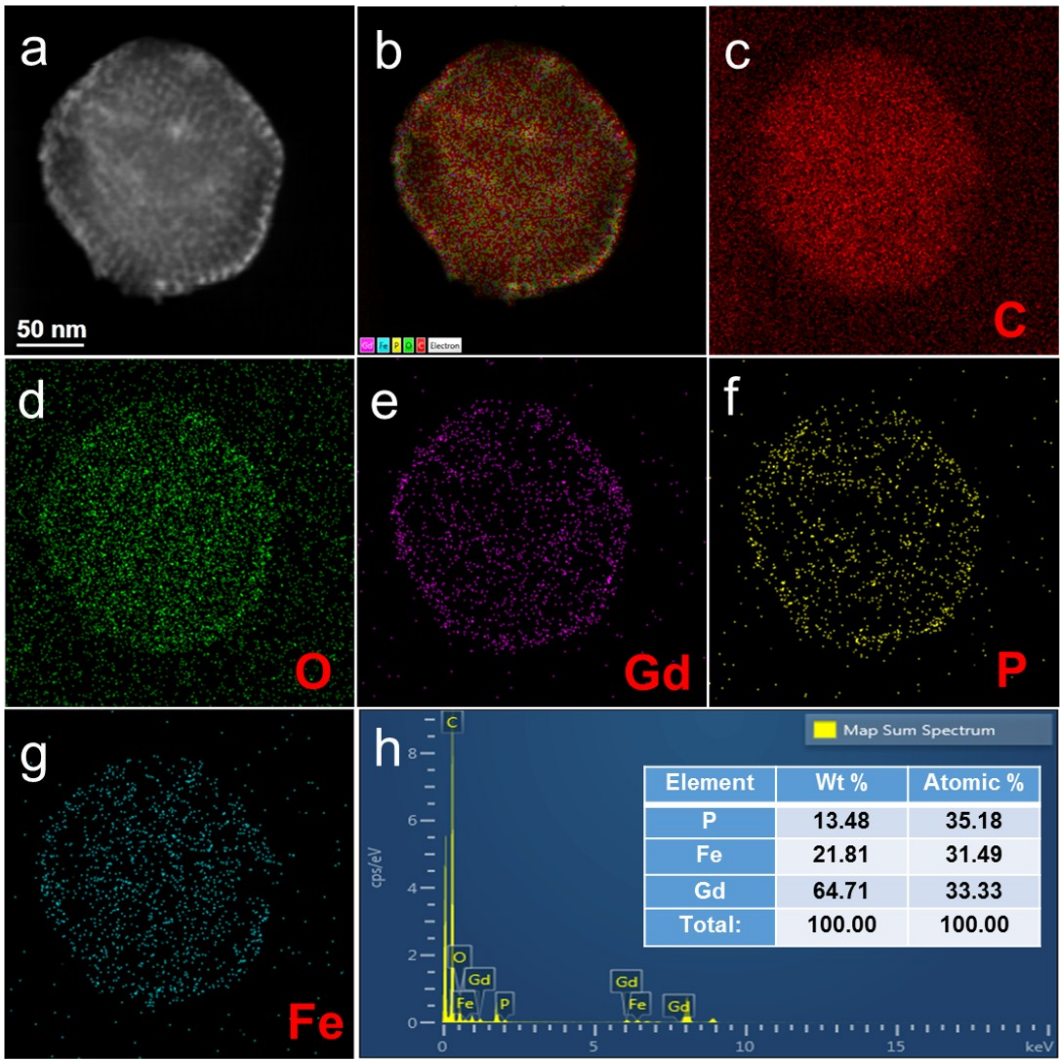

Figure S11. XPS patterns of Fe–Gd/OMCS-*n*: (I) Fe–Gd/OMCS-15, (II) Fe–Gd/OMCS-30, (III) Fe–Gd/OMCS-45, (IV) Fe–Gd/OMCS-60 and (V) Fe–Gd/OMCS-75.

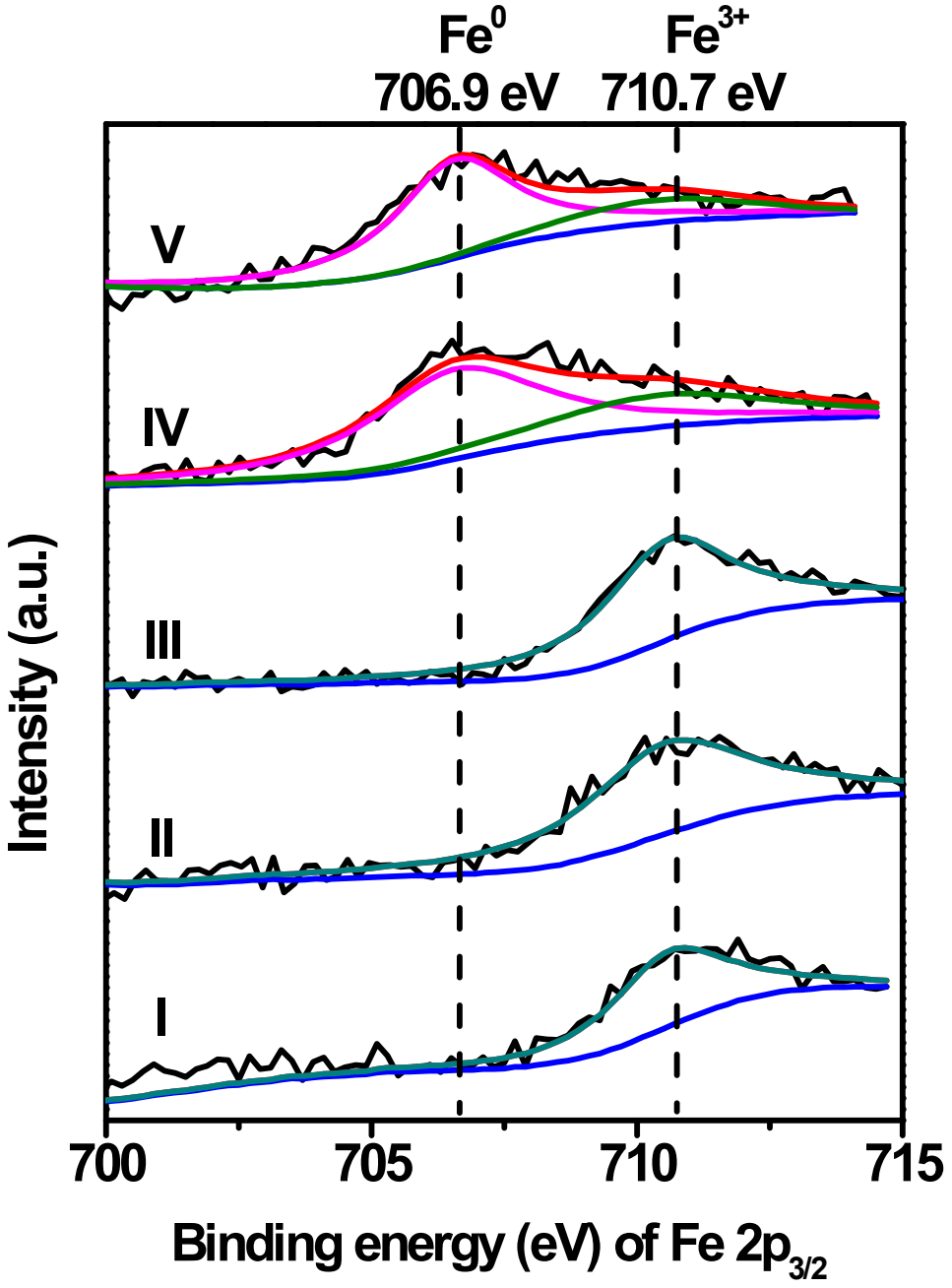

Figure S12. (a) PXRD and (b) XPS patterns of Fe–Gd/OMCS-45-*T* (*T*: carbonization temperature (°C)): (I) Fe–Gd/OMCS-45-700, (II) Fe–Gd/OMCS-45-800.

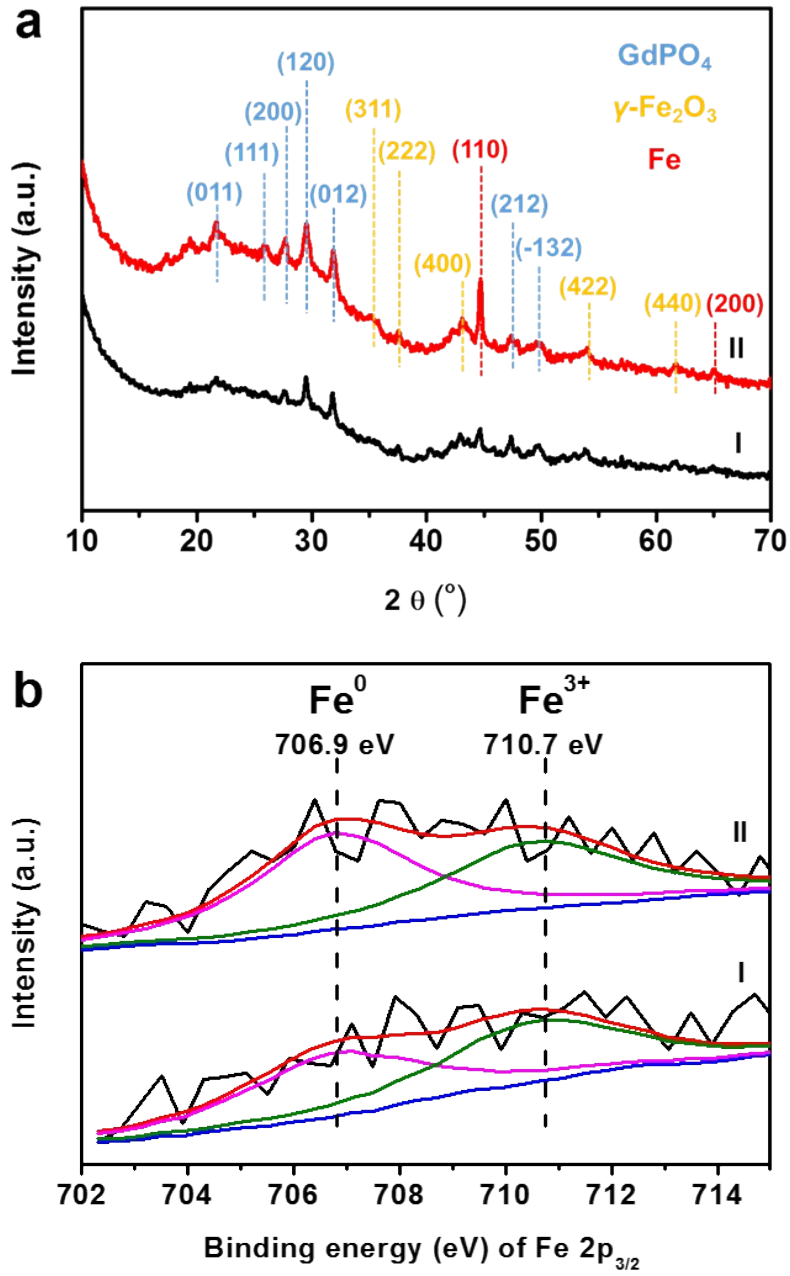

Figure S13. TEM images of Fe–Gd/OMCS-45-*T* (*T*: carbonization temperature (°C)): (a) Fe–Gd/OMCS-45-700, (b) Fe–Gd/OMCS-45-800.

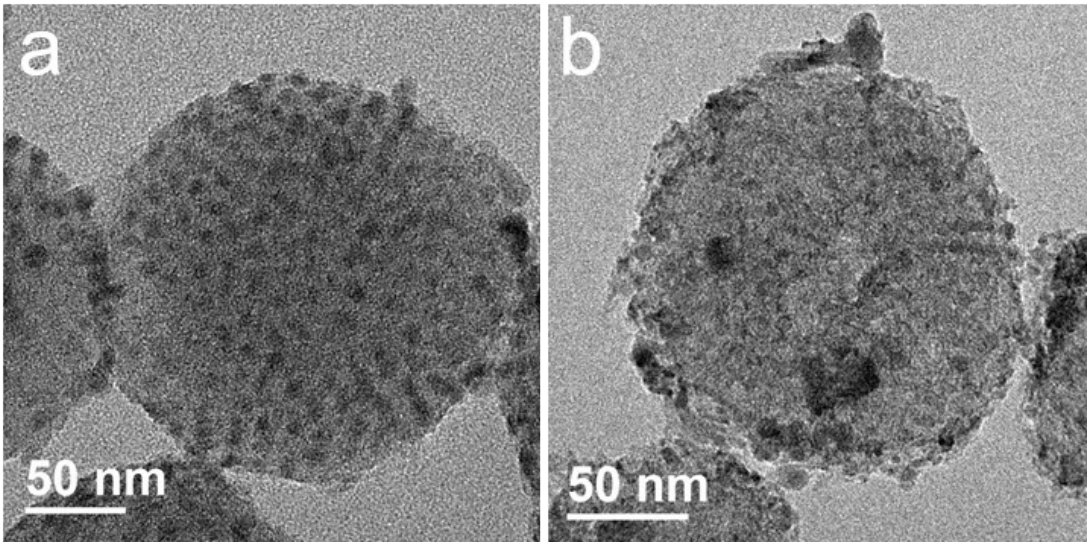

Figure S14. SAXS patterns of (I) as-made mesostructured polymers (Fe–Gd/OMCS-45-i-as-made) and (II) Fe–Gd/OMCS-45-i.

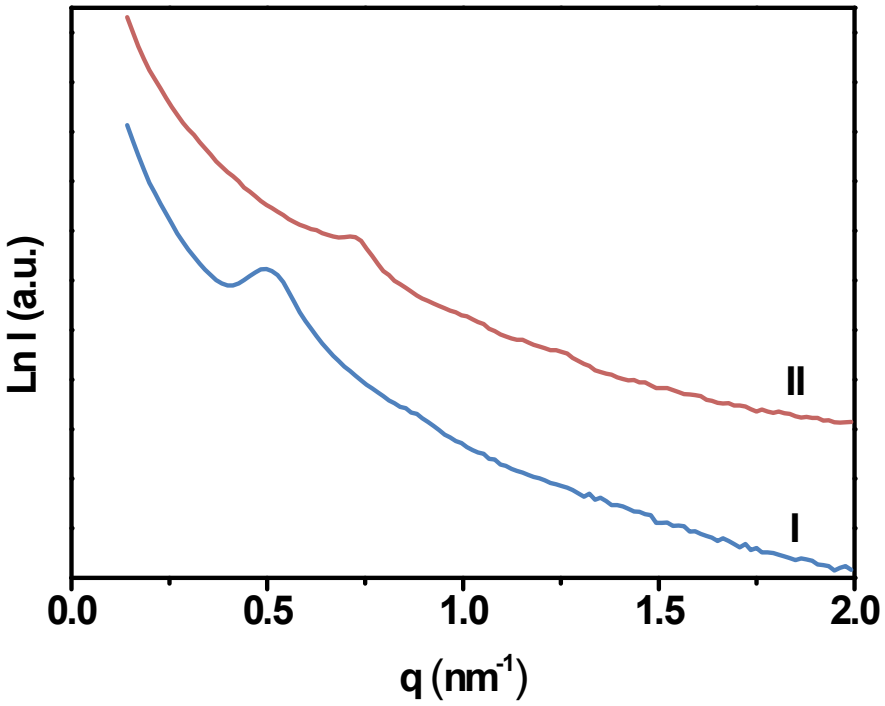

Figure S15. Fe–Gd/OMCS-45-i composites: (a) TEM image, (b)HAADF-STEM image, (c) overlay maps of C, O, Gd, P and Fe elements, the corresponding EDS maps of (d) O, (e) Gd, (f) P, (g) Fe and (h) the corresponding element analysis result.

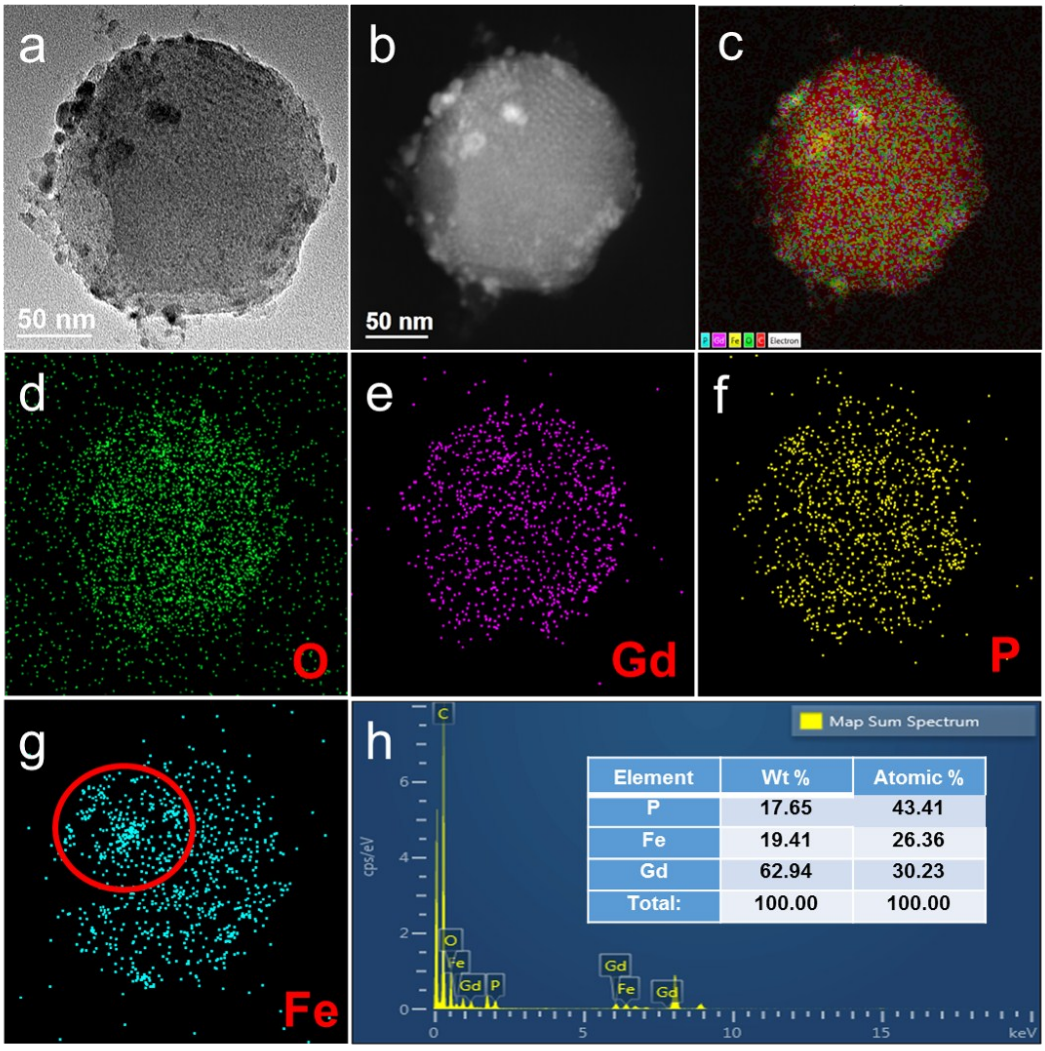

Element	Wt %	Atomic %
P	17.65	43.41
Fe	19.41	26.36
Gd	62.94	30.23
Total:	100.00	100.00

Figure S16. PXRD pattern of Fe–Gd/OMCS-45-i.

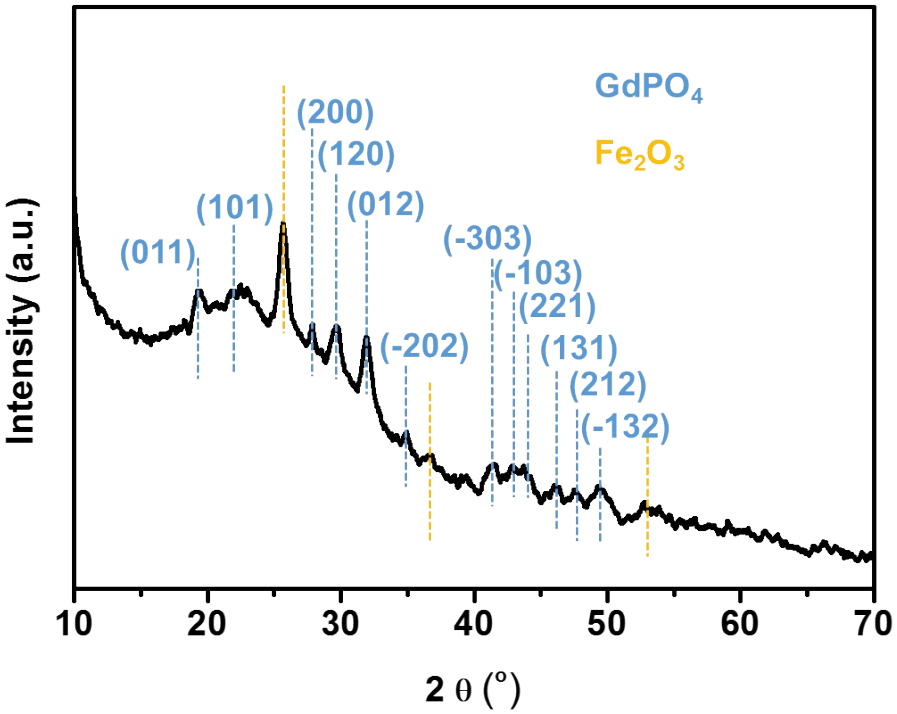

Figure S17. (a) SAXS patterns of (I) as-made mesostructured polymers (F127/resol), (II) OMCSs, (III) Fe–Gd/OMCS-45-ii. (b) PXRD pattern of Fe–Gd/OMCS-45-ii.

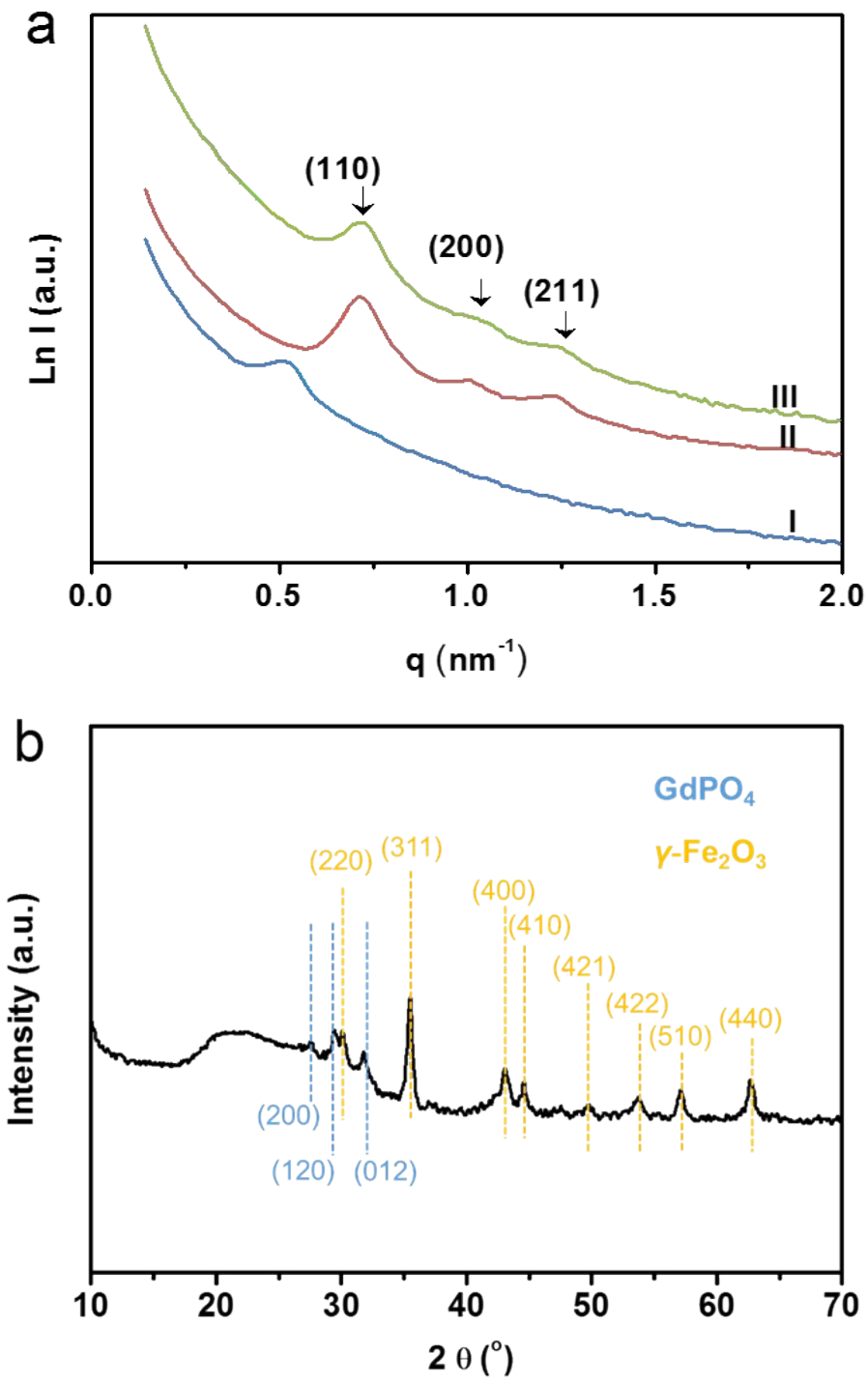

Figure S18. TEM images of Fe–Gd/OMCS-45-ii.

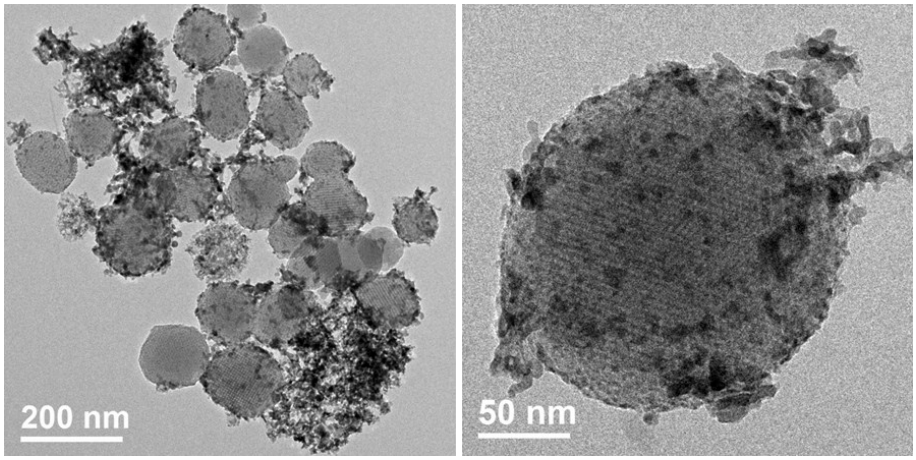

Figure S19. SAXS patterns of (I) Fe–Gd/OMCS-45, (II) Fe–Gd/OMCS-45-air.

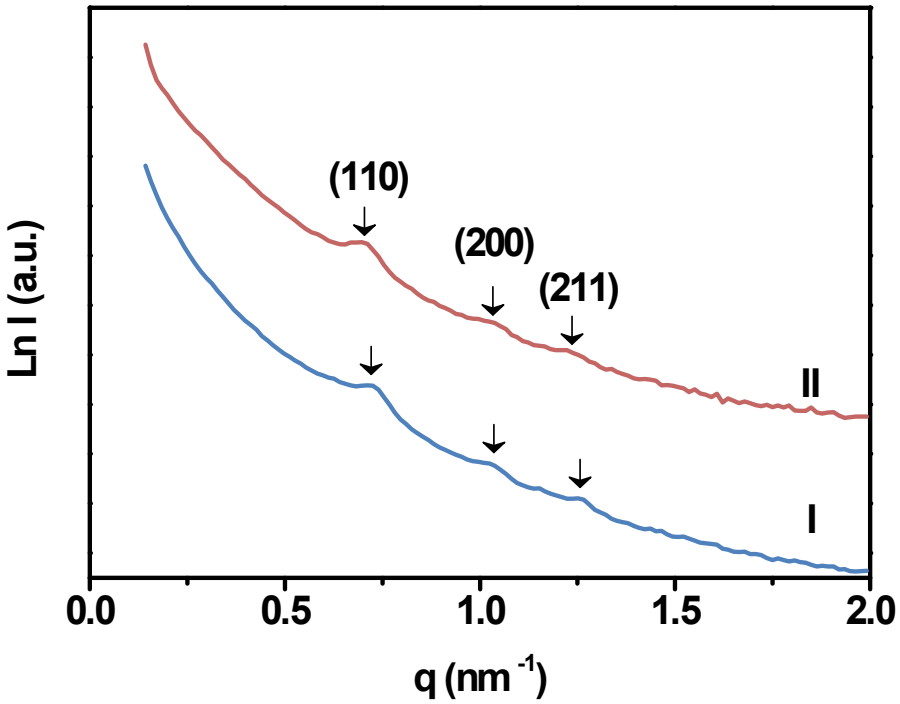

Figure S20. TEM image and elemental analysis result of Fe–Gd/OMCS-45-air.

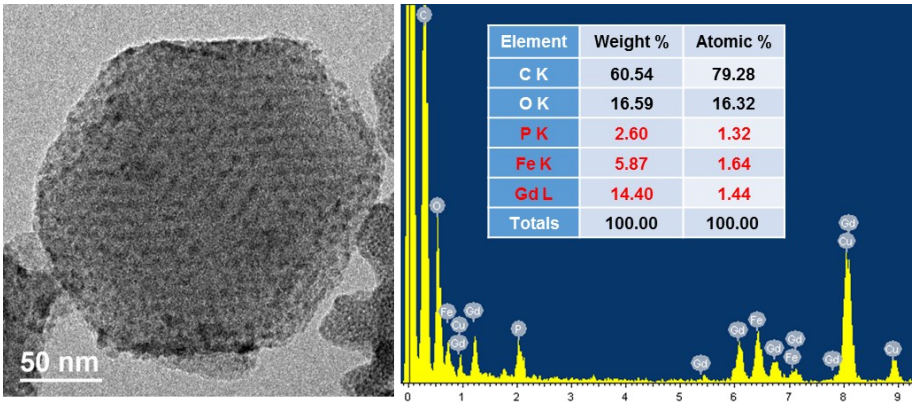

Figure S21. (a) FT-IR absorption spectra of Fe–Gd/OMCS-45 and Fe–Gd/OMCS-45-air. (b) the solubility of Fe–Gd/OMCS-45 (left) and Fe–Gd/OMCS-45-air (right) in aqueous solution.

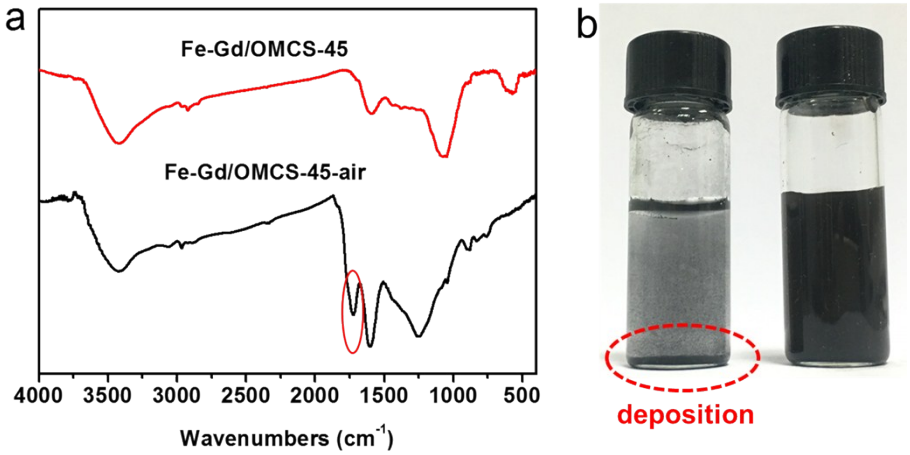

Figure S22. Adsorption amount of DOX functioned with the soak times of Fe–Gd/OMCS-45-air in DOX solution (1 mg ml^{-1}) at room temperature.

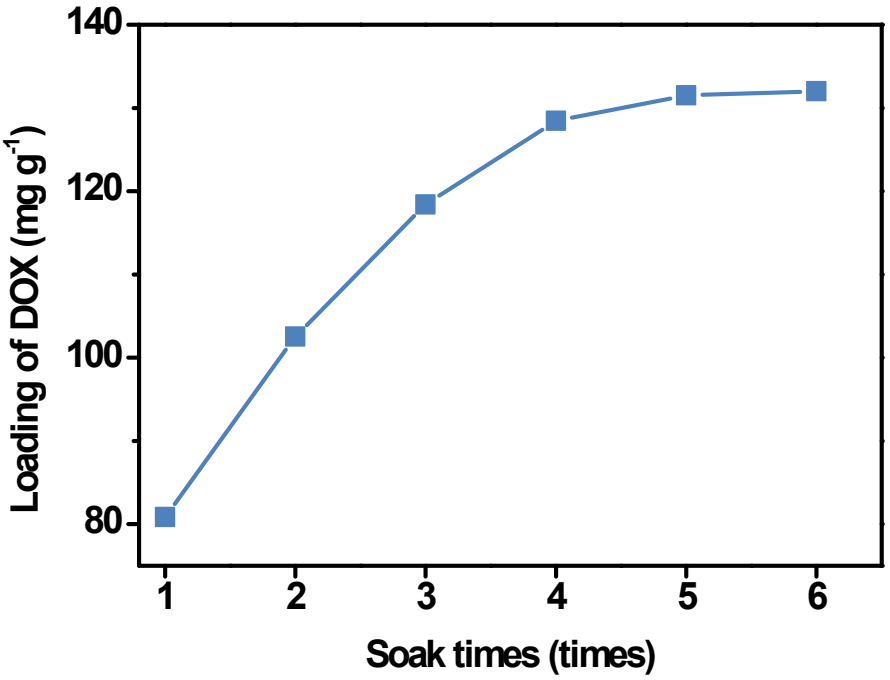

Figure S23. Cellular viability of HeLa cells with Fe–Gd/OMCS-45-air (black) and DOX@Fe–Gd/OMCS-45-air (red) incubation at different concentrations for 4 h (a), for 24 h (b).

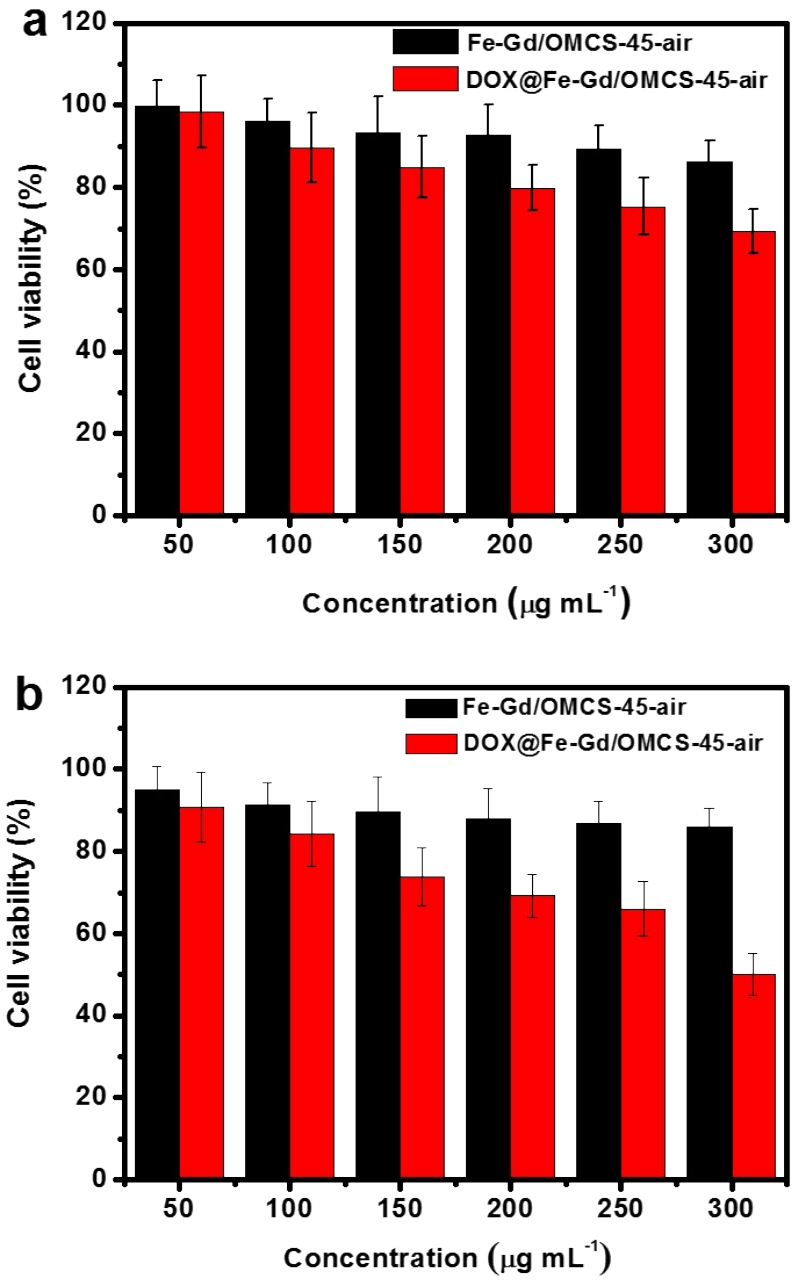

Figure S24. (a) T_1- and (b) T_2-weighted MR images of DOX@Fe–Gd/OMCS-45-air in Hela cells at various concentration (from left to right, 0 μg ml^{-1}, 50 μg ml^{-1}, 100 μg ml^{-1}) after incubation for 4 h on 0.5 T MR system.

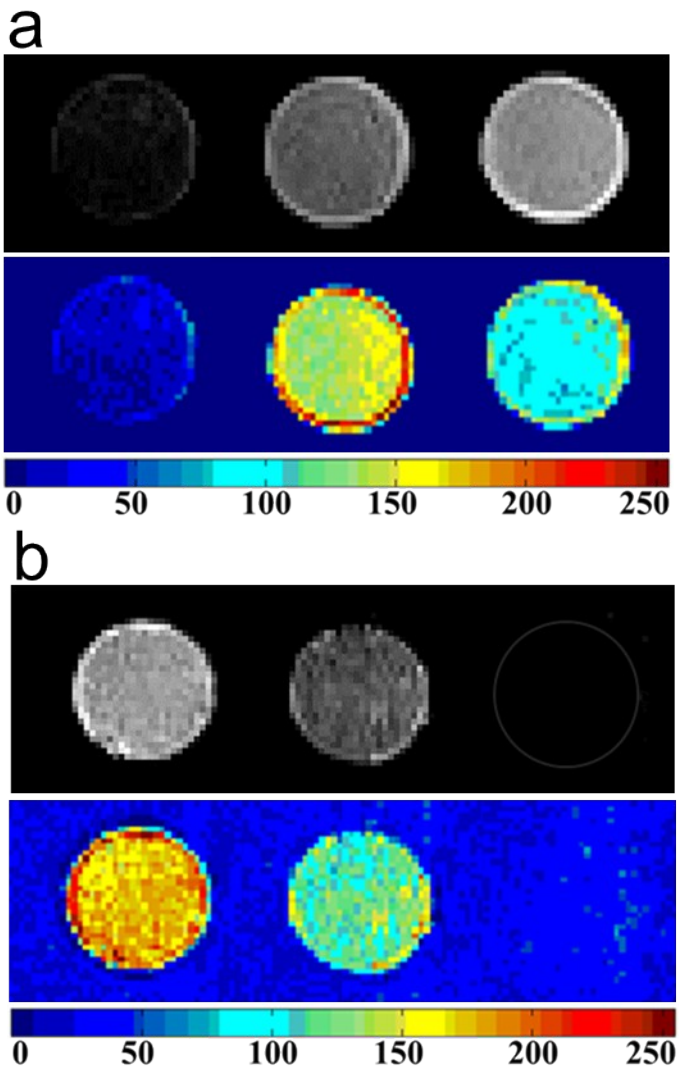

Table S1. The leaching testing results of Fe–Gd/OMCS-45-air in PBS solution.

Fe–Gd/OMCS-45-air	In PBS solution	
Element	Fe	Gd
The content (ppm)	0.001	0.001

The leaching testing of the Fe–Gd/OMCS-45-air in PBS solution: 5 mg of Fe–Gd/OMCS-45-air materials were dispersed in 5 mL of PBS solution. Then the mixture was quiescent at 37 °C for 4 h. After that, the mixture was centrifuged by 10000 rpm/min for 10 min and the supernatant was collected. The contents of Fe and Gd in the supernatant were determined by ICP-AES analysis.

Table S2. Relaxivities and drug loading of different multifunctional nanospheres.

Sample	MR imaging		Drug Loading (mg g^{-1})	Reference
	r_1 (mM^{-1} s^{-1})	r_2 (mM^{-1} s^{-1})		
Fe–Gd/OMCS-45-air	8.2 (0.5 T)	94.3 (0.5 T)	132 (DOX)	This work
Mesoporous Fe_3O_4 nano/microspheres	-	36.3 (1.5 T)	74.5 (Buprofen)	7
HMMNS–R/Ps (Fe_2O_3, SiO_2)	-	124.3 (3.0 T)	150 (DOC) 140 (CPT)	8
Magnetic mesoporous silica nanospheres	-	15.4 (0.5 T)	150 (DOX)	9
γ-Fe_2O_3/Silica spheres/Au	-	1.825 (7 T)	23 (DOX)	10
Fe_3O_4 rattle-type silica	-	138.5 (3.0 T)	500 (Docetaxel)	11
Hollow and porous $GdVO_4$: Dy^{3+} spheres	0.3716 (0.5 T)	-	110 (DOX)	12
$BaGdF_5$ nanospheres	2.132 (1.5 T)	-	251 (MH)	13
Fe_3O_4@dual mesoporous silica spheres	-	421.5 (3.0 T)	650 (DOX)	14
Rattle-type Fe_3O_4 mesoporous silica nanosphere-PEG/FA	-	171.0 (3.0 T)	180 (DOC)	15
Hollow mesoporous Eu^{3+}-doped Gd_2O_3	4.49 (1.2 T)	-	310 (DOX)	16
PEG/Mn-doped hollow mesoporous silica nanoparticles	2.46 (1.5 T)	-	780 (DOX)	17
Fe_3O_4@Mesoporous silica	-	245 (1.5 T)	-	18

References

1. F. Q. Zhang, Y. Meng, D. Gu, Y. Yan, Z. X. Chen, B. Tu and D. Y. Zhao, *Chem. Mater.*, 2006, **18**, 5279–5288.
2. E. M. Pineda, F. Tuna, Y. Z. Zheng, S. J. Teat, R. E. P. Winpenny, J. Schnack and E. J. L. Mcinnes, *Inorg. Chem.*, 2014, **53**, 3032–3038.
3. E. I. Tolis, M. Helliwell, S. Langley, J. Raftery and R. E. P. Winpenny, *Angew. Chem. Int. Ed.*, 2003, **42**, 3804–3808.
4. N. V. Gerbeleu, A. S. Batsanov, G. A. Timko, Y. T. Struchkov, K. M. Indrichan, G. A. Popovich, *Dokl. Akad. Nauk SSSR*, 1987, **293**, 364–367.
5. T. A. Zoan, N. P. Kuzmina, S. N. Frolovskaya, A. N. Rykov, N. D. Mitrofanova, S. I. Troyanov, A. P. Pisarevsky, L. I. Martynenko and Y. M. Korenev, *J. Alloys Compd.*, 1995, **225**, 396–399.
6. Y. Fang, D. Gu, Y. Zou, Z. X. Wu, F. Y. Li, R. C. Che, Y. H. Deng, B. Tu and D. Y. Zhao, *Angew. Chem. Int. Ed.*, 2010, **49**, 7987–7991.
7. S. H. Xuan, F. Wang, J. M. Y. Lai, K. W. Y. Sham, Y. -X. J. Wang, S. -F. Lee, J. C. Yu, C. H. K. Cheng and K. C. -F. Leung, *ACS Appl. Mater. Inter.*, 2011, **3**, 237–244.
8. H. X. Wu, S. J. Zhang, J. M. Zhang, G. Liu, J. L. Shi, L. X. Zhang, X. Z. Cui, M. L. Ruan, Q. J. He and W. B. Bu, *Adv. Funct. Mater.*, 2011, **21**, 1850–1862.
9. H. X. Wu, L. H. Tang, L. An, X. Wang, H. Q. Zhang, J. L. Shi and S. P. Yang, *React. Funct. Polym.*, 2012, **72**, 329–336.
10. K. Rudzka, A. V. Delgado and J. L. Viota, *Mol. Pharm.*, 2012, **9**, 2017–2028.
11. L. Qiang, X. W. Meng, L. L. Li, D. Chen, X. L. Ren, H. Y. Liu, J. Ren, C. H. Fu, T. L. Liu, F. P. Gao, Y. Q. Zhang and F. Q. Tang, *Chem. Commun.*, 2013, **49**, 7902–7904.

12. X. J. Kang, D. M. Yang, P. A. Ma, Y. L. Dai, M. M. Shang, D. L. Geng, Z. Y. Cheng and J. Lin, *Langmuir*, 2013, **29**, 1286–1294.

13. Q. Zhao, Z. Lei, S. Huang, X. L. Han, B. Q. Shao, W. Lü, Y. C. Jia, W. Z. Lv, M. M. Jiao, Z. X. Wang and H. P. You, *ACS Appl. Mater. Inter.*, 2014, **6**, 12761–12770.

14. X. F. Luo, D. C. Niu, Y. Wang, Y. G. Zhai, J. Z. Chen, J. L. Gu, J. L. Shi and Y. S. Li, *RSC Adv.*, 2015, **5**, 39719–39725.

15. H. X. Wu, G. Liu, S. J. Zhang, J. L. Shi, L. X. Zhang, Y. Chen, F. Chen and H. R. Chen, *J. Mater. Chem.*, 2011, **21**, 3037–3045.

16. H. -Z. Shi, L. Li, L. -Y. Zhang, T. -T. Wang, C. -G. Wang and Z. -M. Su, *Dyes Pigments*, 2015, **123**, 8–15.

17. L. D. Yu, Y. Chen, M. Y. Wu, X. J. Cai, H. L. Yao, L. L. Zhang, H. R. Chen and J. L. Shi, *J. Am. Chem. Soc.*, 2016, **138**, 9881–9894.

18. J. Kim, H. S. Kim, N. Lee, T. Kim, H. Kim, T. Yu, I. C. Song, W. K. Moon and T. Hyeon, *Angew. Chem. Int. Ed.*, 2008, **47**, 8438–8441.